

R8902063 ←

STRUCTURE AND RADIATION PROPERTIES OF LARGE TWO PHASE FLAMES

by

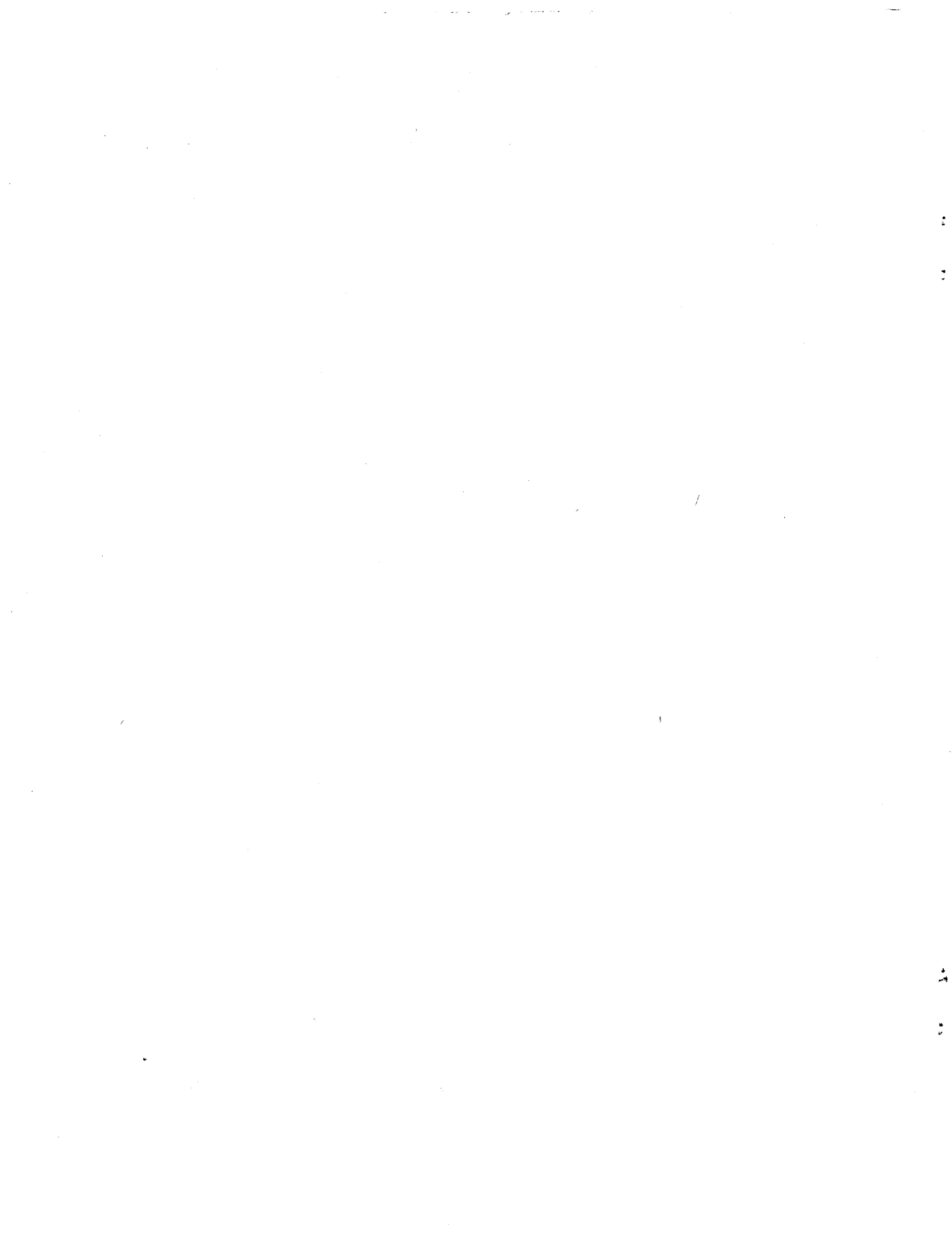
J.P. Gore, S.M. Skinner
Department of Mechanical Engineering
University of Maryland
College Park, MD 20742

and

D.W. Stroup, D. Madrzykowski, and D.D. Evans
Center for Fire Research
National Institute of Standards and Technology
Gaithersburg, MD 20899

IN: American Society of Mechanical Engineers (ASME). Heat Transfer in Combustion Systems. Winter Annual Meeting. HTD-Vol. 122. December 10-15 1989, San Francisco, CA. Ashgriz, N., Quintiere, J.G., Semerjian, H.G. and Slezak, S.E., Editor(s), 1989.

NOTE: This paper is a contribution of the National Institute of Standards and Technology and is not subject to copyright.



STRUCTURE AND RADIATION PROPERTIES OF LARGE TWO PHASE FLAMES

J.P. Gore, S.M. Skinner
Department of Mechanical Engineering
The University of Maryland
College Park, MD 20742*

D.W. Stroup, D. Madrzykowski and D.D. Evans
Center for Fire Research
National Institute of Standards and Technology
Gaithersburg, MD 20899

ABSTRACT

Measurements and predictions of temperatures and radiation for large two-phase, non-premixed flames burning heptane or crude oil and methane in air are reported. Analysis involves the locally-homogeneous flow approximation (LHF), a k-e-g turbulence model and the conserved scalar formulation. State relationships for the mixtures are estimated from those of the individual fuels. Radiative heat fluxes are obtained using the discrete transfer method and narrow band analysis. Methane/air flames are studied as a baseline. The analysis underpredicts the temperatures by ten percent and the heat fluxes by thirty percent for the two phase flames.

NOMENCLATURE

d	burner exit diameter
f	mixture fraction
g	square of mixture fraction fluctuations
H	total enthalpy (chemical + sensible)
h^0_{fi}	heat of formation of species i
h_i	sensible energy of species i
k	turbulent kinetic energy
m	burner mass flow rate
N	number of product species
Q	chemical energy release
Re	burner exit Reynolds number
Ri	burner exit Richardson number
T	temperature
u	streamwise velocity
u_0	equivalent streamwise velocity at the burner exit
x	height above the burner
X_r	radiative heat loss fraction
Y_i	mass fraction of species i
e	rate of dissipation of turbulence kinetic energy

INTRODUCTION

Faeth (1977, 1983, 1988) has reviewed current analyses of combustng sprays. Past work has generally been restricted to the consideration of liquid sprays injected into combustion environments with pressure- or air-atomization. Radiation from such spray flames has been considered using multflux approximations by some investigators (Gosman and Ioannides, 1981; Gosman et al., 1980; Swithenbank et al., 1980; Mongia and Smith, 1979) while neglected by others (El Banhawy and Whitelaw, 1980; Butler et al., 1980). All of these investigators have either used chemical equilibrium or global Arrhenius expressions to model the flame chemistry. The limitations of such an approach in turbulent environments have been described by Bilger (1977).

Grosshandler and Sawyer (1978) have studied radiation properties of methanol/air combustion products in a test furnace. They have also developed an algorithm for calculating flame radiation (RADCAL). This algorithm is based on the narrow-band model and the Curtis-Godson approximation following Ludwig et al. (1973). Grosshandler and Sawyer (1978) have used measurements of flame structure properties to obtain predictions of radiation intensities. Karman and Steward (1984) have studied the radiation properties of flames burning a mixture of propane and propylene with air. They have reported the enhancement of radiation by adding approximately 7 % by weight (of fuel) of carbon particles to the fuel and air streams. Karman and Steward (1984) have also used measurements of structure properties to obtain encouraging radiation predictions using RADCAL.

Shuen et al. (1986) report a study of an ultra-dilute spray formed by injecting methanol droplets in a methane flame. They state that the droplet concentrations in this study were so small that the flame structure is completely determined by the gaseous methane flame. Radiation properties of the spray flames are not reported but are probably not very different from those of the pure methane flame studied by Jeng and Faeth (1984).

Keywords: Fires/Flames, Multiphase Flows, Radiation
*Work performed at the Center for Fire Research, National Institute of Standards and Technology.

Several papers have addressed the structure and radiation properties of turbulent non-premixed gaseous jet flames (Gore et al., 1987 a,b; Jeng and Faeth, 1984; Gore and Faeth, 1986,1988; and Gore, 1988). All of these studies considered single phase gaseous fuels injected into still air. Recently Gore et al.(1988) considered the effects of addition of liquid water into natural gas flames. In practical applications such as spray flames and fires resulting from oil well blowouts, the fuel jet may consist of a two-phase mixture. The objective of the present study is to extend the past analysis to the treatment of structure and radiation properties of flames burning two-phase mixtures.

A spray of either n-heptane or Alberta sweet crude oil is generated by twin-fluid atomization with part of the methane. The atomization is aided by a coflow of the main methane which is also used to control the mass ratio of the two fuels. Overall heat release rates are nominally 15 MW. Measurements of flame temperatures and radiative heat fluxes to target locations are obtained.

Theoretical analysis is limited to the locally homogeneous flow (LHF) approximation of multiphase flow theory. Since details of the initial conditions for the present test flames are not precisely known, this is the most logical first step (Faeth, 1988). Even if separated flow calculations are considered, data concerning separate properties of the two phases could not be obtained in the present large scale flames. Within the LHF approximations, flame structure is treated using the conserved scalar formalism and the laminar flamelet concept. State relationships for the present two phase mixture of fuels are not available. Therefore, these are constructed using the state relationships for individual fuels. On the fuel-lean side this amounts to assuming that the two fuels react independently. On the fuel-rich side, there is additional ambiguity concerning the sharing of oxygen between the two fuels.

Once the flame structure is known, the radiation properties are calculated using RADCAL. The scattering of radiation by liquid fuel drops is neglected as a first step. In the present analysis, liquid particles can exist only in a small cold interior portion of the spray flame. Therefore, this assumption is consistent.

In the following, the experimental methods and conditions are summarized. The analysis of flame structure and radiation properties is then described. Finally, results of the experiments and the calculations are discussed.

EXPERIMENTAL METHODS

Apparatus

The tests are conducted outdoors since the flame heights are approximately 10 meters. The construction of the burner is similar to the one used by McCaffrey(1986). Figure 1 shows a sketch of the experimental apparatus with details of the burner. A twin fluid atomizer (Spraying Systems Inc., model 1J, spray setup 172, fluid nozzle No. 6251000, air cap no. 11251625)[†] is used to inject the liquid fuel (either n-heptane or Alberta sweet crude oil) into a coflow of methane. The coflow

tube is 102 mm in diameter with a 50.4 mm diameter 45° sharp-edged orifice plate at the exit. The atomizer assembly is located at a depth of 52 mm from the orifice exit. The coflow of methane is obtained from a "fuel supply tube trailer" which has several 8 meter long commercial gas cylinders in parallel. The main gas flow is metered using an orifice plate and a pressure drop transducer. The gas temperature used in the calculation of the flow rate is measured at the orifice plate using a thermocouple. Atomizing methane gas is obtained from an A1 size commercial gas cylinder. The atomizing gas is metered using a rotameter. Liquid heptane or crude oil is pumped into a vessel and then pressurized using bottled nitrogen. The flow rate of liquid fuels is monitored using a rotameter. The liquid flow is maintained constant by controlling the pressure in the vessel by adding nitrogen as the liquid level decreases. The burner can be operated for about 5 minutes with the present arrangement.

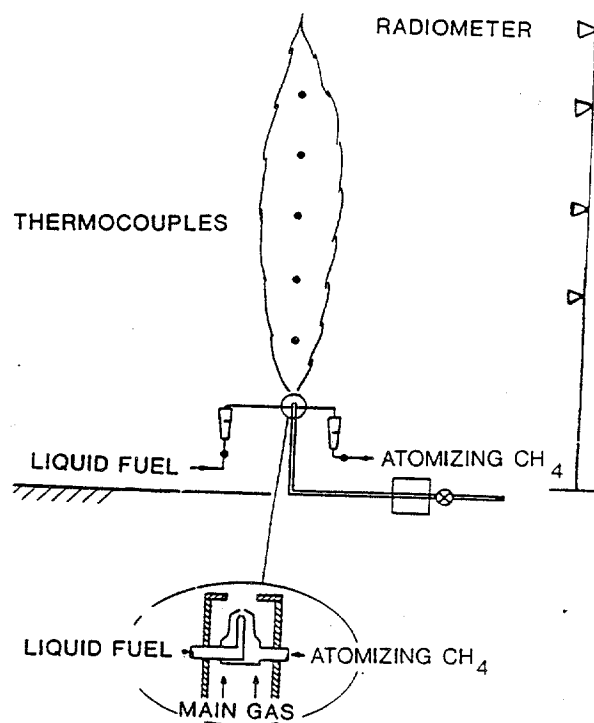


Fig. 1 Sketch of Experimental Apparatus

Instrumentation

Measurements of flame temperatures at five representative locations(see Figure 1) along the axis of the flames are obtained using type K thermocouples. These are made by joining uncoated 0.5 mm diameter chromel-alumel wires. Steel wires

[†]Commercial equipment is identified in this paper for adequately specifying experimental procedure. Such identification does not imply recommendation or endorsement by the National Institute of Standards and Technology nor does it imply that the equipment is necessarily the best available for the purpose.

strung between two vertical beams are used to support the thermocouples in the flames. Radiative heat fluxes perpendicular to the axis of the flames are monitored using four water cooled wide angle radiometers (Medtherm Corp., 150° view angle). The radiometers are mounted on a vertical mast at 6.8 meters from the flame axis. A separate radiometer is used to monitor the background radiation since the tests are conducted in an open field. Ambient temperature is also recorded using a thermocouple. The six thermocouple channels, the six radiometer channels the pressure transducer channel are continuously monitored and stored during the tests using a datalogger and a laboratory computer. Each channel is recorded approximately every five seconds. Ambient wind speed is measured. No visible effects of ambient wind are observed when the speed is below 1.0 m/s. Wind speeds of 0.2 to 0.5 m/s are typically observed during the tests.

Operating Conditions

Five fully instrumented tests are reported. The test conditions are summarized in Table 1. Tests 1-3 involve liquid heptane while tests 4 and 5 involve Alberta sweet crude oil. The Reynolds numbers at the exit are for both single phase and two phase operation, giving fully turbulent flames. The Richardson numbers are low at the injector exit, but based on the criteria of Becker and Liang (1978), the flames are affected by buoyancy. A photograph of a typical flame burning the two phase fuel mixture is shown in Figure 2.

Table 1: Summary of Test Conditions

Test	m _{CH4a} Kg/s	m _{ljq} ^a Kg/s	u _{0b,c} m/s	Re ^c x10 ⁻⁵	Ri ^c x10 ⁵	Q _{CH4} MW	Q _{Tot} MW
1	0.16	0.22	121	3.0	3.4	8.0	17.6
2	0.17	0.22	129	3.2	3.0	8.5	18.1
3	0.16	0.22	121	3.0	3.4	8.0	17.6
4	0.17	₋ d	129	3.2	3.0	8.5	₋ d
5	0.16	₋ d	121	3.0	3.4	8.0	₋ d

^acommercial grade.

^bcalculated using actual injector diameter and the total mass flow.

^cunder the present approximation, these quantities are identical for the single-phase and the two-phase flames.

^dthese quantities were not calculated for the crude oil/methane flames.

The flame in Figure 2 appears vertical and symmetric. The visible flame height in Figure 2 is approximately 7 meters. The flames appear to be lifted from the injector exit.

Test Procedure

The tests are started by lighting a small pilot flame of methane. The main and atomizing methane flows are then started and stabilized at the single-phase operating conditions summarized in Table 1 for about one minute. The flow of liquid fuel is then started and stabilized at the two-phase operating conditions for about one minute. Thus, during each test, data for a single phase methane flame and a two phase methane-liquid fuel flame are generated.

THEORETICAL METHODS

The important features of the analysis can be demonstrated using the pure methane and methane+n-heptane flames due to the relative simplicity of these fuels. Comparative experimental data for the Alberta sweet crude oil are presented without analysis.



Fig. 2. Photograph of a Heptane-Methane Flame

Flame Structure

The flame structure analysis is considerably simplified via the locally homogeneous flow (LHF) approach. Under this approximation the multiphase flame reduces to a variable property, single phase reacting flow. Further simplification is achieved when the conserved scalar hypothesis together with the laminar flamelet concept can be utilized. The conserved scalar hypothesis implies that all scalar properties are unique functions, called state relationships by Faeth and Samuelsen (1986), of a conserved scalar such as the local instantaneous mixture fraction. The mixture fraction is defined as the fraction of the mass at any location that originated in the fuel stream. The laminar flamelet concept allows the determination of state relations from laminar flame experiments or calculations. Since the density changes substantially, Favre averaging following Jeng and Faeth(1984) is adapted. The effects of liftoff are neglected due to considerable uncertainties in the current understanding (Pitts, 1988).

Within the above approximations, a previously calibrated k-e-g turbulence model is used (Jeng and Faeth, 1984). Solution of the governing equations for mass, axial momentum and mixture fraction together with the modelled equations of turbulence kinetic energy, dissipation and mixture fraction fluctuations is obtained. All turbulence constants

are unchanged from those of Jeng and Faeth (1984). The specification of state relationships for two phase mixture of fuels is the main task in the present theoretical work.

Once the state relationships are known, mean values of any scalar property can be found using a probability density function of mixture fraction. Within the present turbulence model only two parameter probability density functions can be treated. Following past practice (Jeng and Faeth, 1984), a clipped Gaussian form is selected.

Initial Conditions

Past laboratory studies have used experimental measurements to specify initial conditions. For the present large scale outdoor flames, this is not feasible due to limitations on resources. The burner design involves injection of a dense spray of liquid in a coflow of gas and subsequent passage of the mixture through a contraction. For the LHF analysis, velocity, density and diameter of a jet equivalent to the conditions produced by the apparatus are needed. This is accomplished by conserving mass and momentum of the incoming streams (Gore et al., 1986). The density of the two-phase mixture is calculated by noting that volumes of the phases are additive.

State Relationships

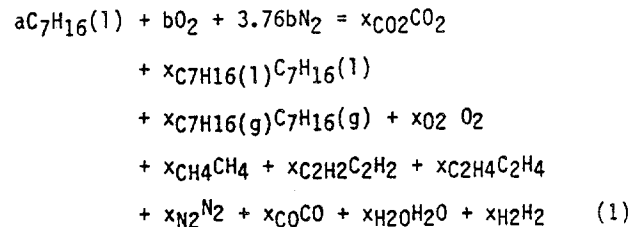
An important task for the present work is the specification of state relationships for the LHF analysis of the two-phase, two-fuel flames. Measurements of species concentrations for n-heptane flames stabilized around porous spheres by Abdel-Khalik et al.(1975) are plotted as a function of local mixture fraction by Bilger(1977) to show that conserved scalar approximation is valid. Therefore, appropriate state relationships for liquid fuels is not an issue in the single phase portions of the spray flame. Measurements of state relationships for fuel rich conditions, which may contain liquid n-heptane, are not available. Faeth(1988) states that these conditions generally involve passive mixing and therefore can be evaluated by simple mixing calculations applied to the relatively lean data. Mao et al.(1980) have demonstrated this approach for a pressure-atomized n-pentane spray burning in air at 3 MPa. The method involves chemical equilibrium calculations for regions with temperature greater than 1000 K and extension to lower temperatures by frozen mixing calculations.

The next issue to be addressed is the construction of state relationships for a fuel mixture given the measurements for individual fuels. Three possibilities exist: (1) Conduct measurements of species concentrations in a laminar flame burning the fuel mixture under consideration; (2) use chemical equilibrium calculations together with frozen mixing, following Mao et al.(1980). However, the choice of the temperature at which the reactions are to be frozen is rather arbitrary; (3) Devise mixing rules for combining the measurements of species concentrations for the two fuels into state relationships for the mixture. The third option is based on the observation that measurements of concentrations of all major species (except carbon monoxide) for the combustion of three different

paraffins; methane and propane (Tsuji and Yamaoka, 1969), methane (Mitchell et al., 1980), and heptane (Abdel-Khalik et al., 1975) can all be expressed in terms of a single state relationship for any paraffin (C_nH_{2n+2}). The failure of such general state relationships for carbon monoxide is not expected to affect the radiation predictions due its minor contribution to the total heat flux. Therefore, in the following, the state relationships for the fuel mixture are constructed using those for pure methane and heptane.

Heptane/Air State Relationships

The measurements of Abdel-Khalik et al.(1975) show that the global chemical reaction for n-heptane burning in air considering major species can be written as:



where the product side contains one mole and x_i represents the mole fraction of species "i". Water vapor and hydrogen are not given by Abdel-Khalik et al.(1975) but are calculated using O/N and C/H ratios. Due to their experimental arrangement, Abdel-Khalik et al.(1975) did not have any liquid heptane in their measurements. In the present calculations liquid heptane is included to obtain state relationships useful for spray calculations. "a" and "b" on the reactant side are to be calculated using atom balances. The additional unknown in equation (1) is the liquid phase mole fraction of heptane. This is evaluated using the vapor pressure relationship given by:

$$\frac{x_{C_7H_{16}(g)}}{(1-x_{C_7H_{16}(l)})} = P_v(T) \quad (2)$$

In order to use the vapor pressure relationship, the temperature of the products must be known. From the conservation of energy for equation (1):

$$\begin{aligned} (1-X_r) \sum_{i=1}^N x_i h_{o fi} R = & \sum_{i=1}^N x_i h_{o fi} p (1-X_r) \\ & + \sum_{i=1}^N x_i \Delta h_i p \end{aligned} \quad (3)$$

where X_r is the radiative heat loss fraction. Similar to past practice a global radiative heat loss fraction is used for all points in the flame (Gore et al., 1986, 1987a,b). Thus each point in the flame loses a fixed fraction of its chemical energy release by radiation. Within this approximation both X_r and the resulting state relationships are independent of the radiative properties (such as optical depth) of the flame.

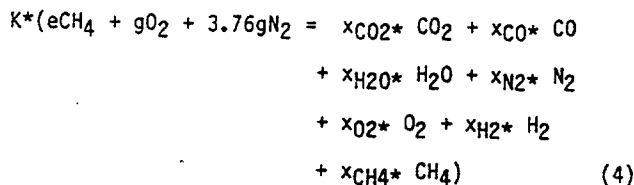
An auxiliary experiment using 50 mm and 75 mm diameter pool flames was completed to obtain the

global radiative heat loss fraction for heptane. Total radiative heat fluxes surrounding these flames were measured using a wide angle radiometer and integrated over an envelope to obtain the energy radiated to the surroundings. The chemical energy release was estimated using the liquid consumption rate and the lower heating value of heptane. Radiative loss fraction, X_r , of 26 % was calculated from these two data. Use of pressure atomized heptane spray flames would be more appropriate for the measurement of radiative loss fraction. However, pool flames are used for their relative simplicity.

Once equations (1)-(3) are solved, the density can be calculated. For the gas phase, the ideal gas law with atmospheric pressure is used to evaluate the density. For the liquid, the density is only a weak function of temperature in the range at which liquid can exist under the LHF approximation. Therefore, a constant density at room temperature is assumed. The density for the two phase mixture is calculated noting that the specific volumes of the two phases are additive.

Methane/Air State Relationships

Gore et al. (1986) have reported measurements of state relationships for natural gas (predominantly methane)/air flames. These are used here to approximate the methane/air combustion. The measurements of major gas species concentration can be summarized as:



Where the product side for the equation inside the parenthesis contains one mole and "e" and "g" are found from atom balances. The multiplication factor K for the whole equation is inserted in order to match the mass ratio of the two fuels in creating state relations for the fuel mixture. There is no possibility of liquid in the products of the present system. Therefore, the temperature and density are evaluated by applying equations (3) and the ideal gas law to each of the measurements represented by equation (4).

State Relationships for the Two-Phase Fuel Mixture

For simplicity, we assume that the chemical reactions for a mixture of fuels proceed independent of each other. The individual state relationships for the two fuels (equations (1) and (4)) are to be combined to obtain the state relationship for fuel mixtures. The ratio of the two fuels in the inlet stream is fixed. This ratio must remain unchanged through the mixing and reaction processes for a mixture state relationship to exist. Therefore from equations (1) and (4):

$$16 Ke/ 100 a = R \quad (5)$$

where "R" is the ratio of mass of methane in the mixture to the mass of heptane. Equations (1) and (4) are sets containing as many individual equations as we choose to obtain from measurements.

In order to add individual equations, we need to establish a correspondence or decide how oxygen is shared by the two fuels. As a first step we start by assuming that individual equations in the sets equation (1) and equation (4) correspond to each other when their mixture fractions are identical:

$$\frac{100 a}{(100a + b(28 * 3.76 + 32))} = \frac{16e}{(16e + g(28*3.76 + 32))} \quad (6)$$

Equations (1), (4)-(6) complete the present approximate rule for construction of state relationships for a mixture given those of the individual fuels.

This procedure corresponds to an implicit assumption that the air is shared by the two fuels in the ratio of their mass. This is only an approximation but a logical first step. Another possibility is that the air is shared in the ratio of the moles of the two fuels. In this case a much leaner methane reaction must be added to a particular heptane reaction. However, any mixing rule of this nature for the state relationships is only approximate and must be verified experimentally.

In addition to the concentrations of the gaseous species, soot concentrations for methane+heptane flames are needed. Past spectral radiation intensity data (Jeng and Faeth, 1984; Gore et al., 1986) for methane flames have shown that the contribution of radiation from soot is negligible. Therefore, it is assumed that the continuum radiation from the methane+heptane flames arises from the soot particles produced by the combustion of heptane. Within the Rayleigh approximation, the only quantities needed for determining the absorption coefficient of soot are its volume fraction and refractive index. The refractive index is obtained from Dalzell and Sarofim (1969). Since measurements of soot volume fractions for the present flames are not available, data from Kent (1987) and Olson et al. (1985) for pure heptane are used to estimate the state relationship for the mixture. The calculation involves simple frozen mixing of the products of heptane with those of methane to calculate a new soot volume fraction assuming that the density of the soot particles remains unchanged. The shape of the state relationship profile for soot volume fractions is assumed to be triangular with a frozen soot region in fuel lean portions similar to that used by Gore and Faeth (1988).

Measurements of X_r for methane+heptane flames are not available. Therefore, an approximate value is estimated by averaging the mass-weighted X_r of the individual fuels.

RESULTS AND DISCUSSION

The state relationships calculated using the procedure discussed above are presented first before discussing the turbulent flame results.

State relationships for methane are shown in Figure 3. Concentrations of major gaseous species are plotted as a function of local mixture fraction. The nominal stoichiometric mixture fraction for methane/air flames is 0.055. The state relationships shown in Fig. 3 are identical to the ones

used by Gore et al.(1986). Mole fractions of all major gas species except water are obtained from measurements. These are shown in Figure 3. The mole fractions of water vapor are calculated by assuming a fixed C/H ratio at all points.

State relationships for liquid heptane burning in air are shown in Figures 4 and 5. Bilger(1977) plotted the state relationships for the gas phase portion. Here, these are extended to the liquid-

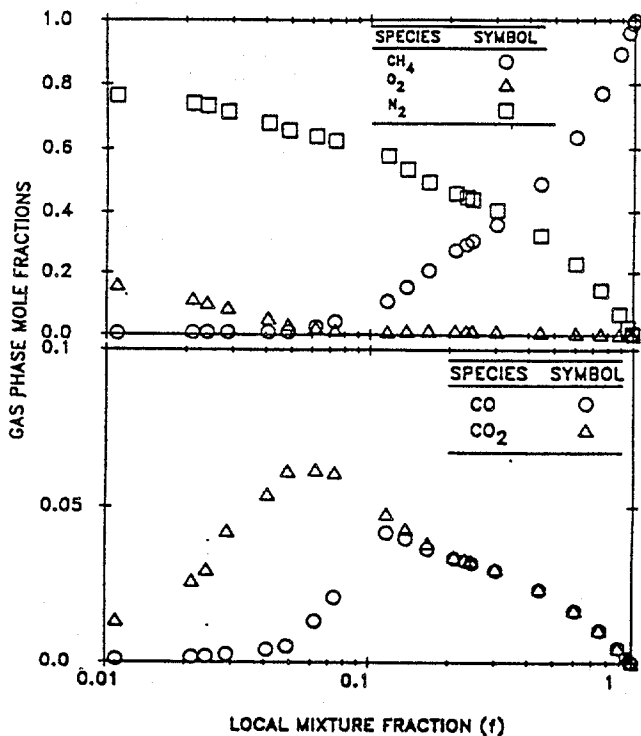


Fig. 3. Methane/Air State Relationships

containing region. Mole fractions of liquid heptane and heptane vapor are plotted as a function of mixture fraction in Figure 4. In constructing these

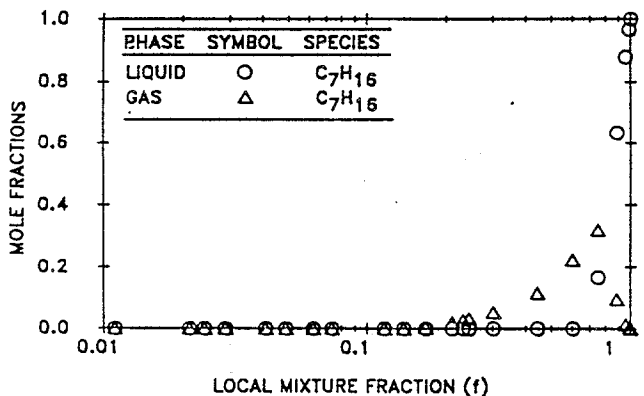


Fig. 4. Heptane Liquid and Vapor State Relationships

state relationships, the measurements are linearly extrapolated to the fuel rich side to obtain the concentrations of heptane (liquid and vapor) and other gas species in the products. Equations (2) and (3) are then used to obtain the temperature and heptane-vapor concentration in the gas phase. The remaining heptane is in the liquid phase. Figure 4 shows that, the concentration of liquid heptane decreases very rapidly. All liquid vanishes at a mixture fraction of 0.6 due to fast transport between the two phases.

Figure 5 shows the state relationships for major gaseous species for heptane used in the present calculation. The mole fractions of all species except heptane are based on the gas phase only. Mole fractions of liquid-vapor heptane are plotted as reference. The mole fractions of gas species increase in regions containing liquid because the total moles in the gas phase decreases.

Figure 6 shows the state relationships for major gas species for a mixture of heptane and methane used in the present experiments (Table 1). These state relationships are obtained by combining those in Figures 3 and 5 using the mixing rule given by equations (5) and (6) together with the

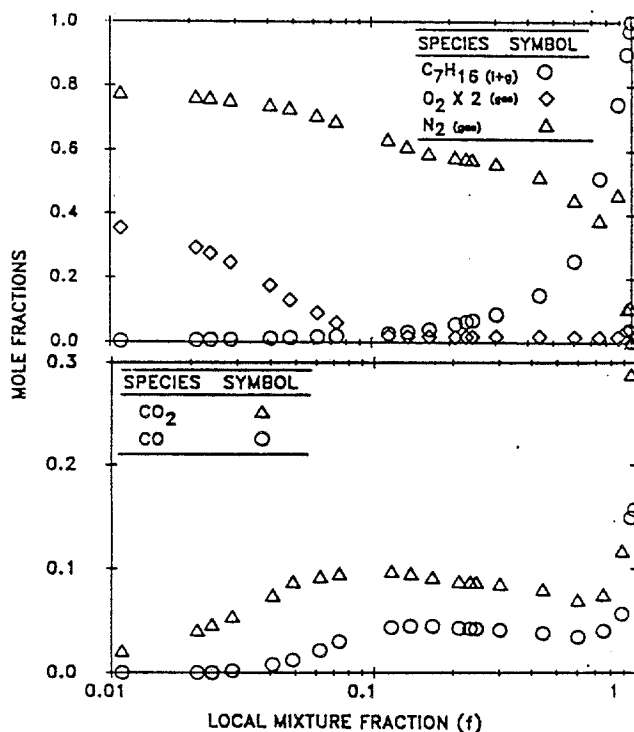


Fig. 5. State Relationships for Heptane/Air Flames

chemical equations (1) and (4). In the inlet fuel stream the mole fraction of liquid heptane is approximately 14%. This liquid rapidly evaporates due to the additional energy release of the gaseous fuel. In fact for the present conditions, all of the liquid fuel evaporates at a mixture fraction of 0.95 as compared to 0.6 for pure heptane. Heptane vapor increases from 0 to approximately 12 percent and then decreases due to pyrolysis and burnout.

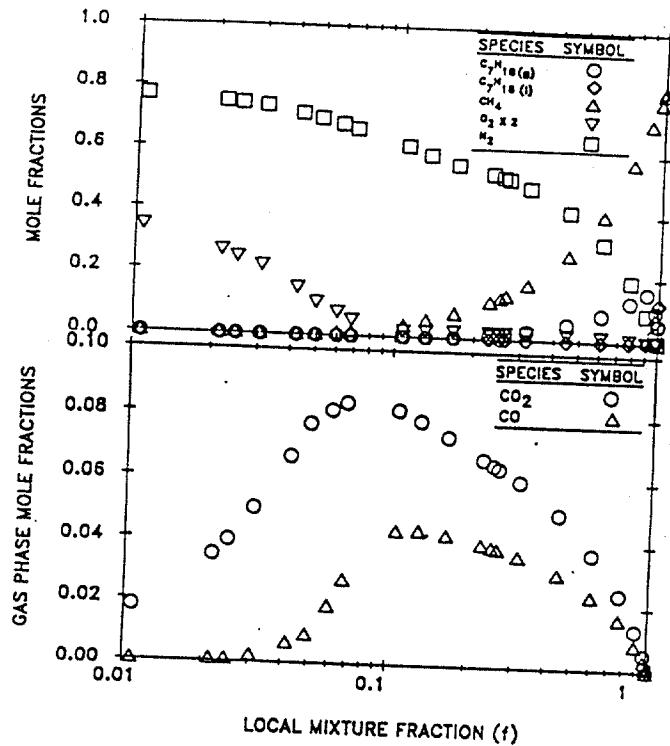


Fig. 6. State Relationships for Mixture of Methane/Heptane burning with Air.

The mole fractions of CO and CO₂ for the mixture are higher than those for pure methane but lower than those for heptane. For paraffins this is expected due to the increase in the C/H ratio as the order increases.

Figure 7 shows the state relationships for temperatures for methane, heptane and the mixture of the two fuels. The stoichiometric mixture fraction for methane (0.055) is lower than that for

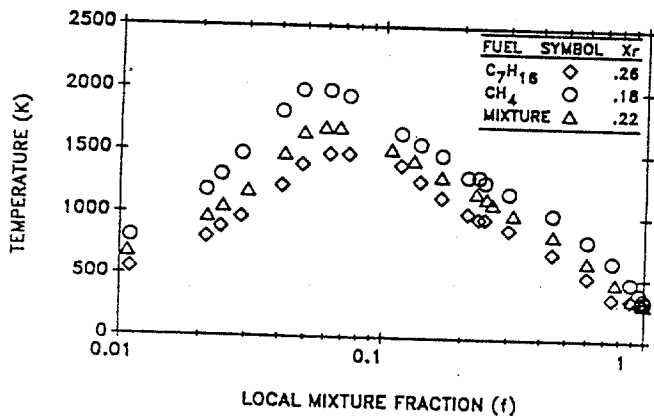


Fig. 7. Temperature State Relationships

heptane (0.062) leading to a peak temperature at a relatively lower mixture fraction. The temperature levels for methane are higher due to:

lower radiation fraction, gas phase at inlet conditions, and higher combustion efficiency. The peak temperature for methane occurs at a mixture fraction close to stoichiometry while for heptane the peak occurs on the fuel rich side. The estimates of temperatures for the pure heptane flames are lower than the measurements of Abdel-Khalik et al. (1975) by about 350 K. This discrepancy is partly due to the higher radiative heat loss fractions for the present flames in comparison with the droplet flames considered in the previous study. Calculations of flame temperatures using equation (3) are also sensitive to changes in the concentrations of species such as CO₂, CO, H₂O and C₇H₁₆.

It is seen from Fig. 7 that, above a mixture fraction of 0.7, the temperature for pure heptane is held relatively low by the vaporization of the liquid fuel. As soon as all the liquid evaporates, the temperature begins to rise. The peak value attained is lower than if heptane vapor was injected into the jet. Within the present approximations, the effects of vaporization of liquid on the temperature profile in the fuel rich region of the mixture flames is small.

The turbulent flame experiments involved heptane or crude oil burning with methane. The heptane tests are conducted to simulate oil well blowouts with a simpler fuel. Measurements of temperature profiles and radiative heat fluxes for both flames are discussed in the following. Predictions for the heptane-methane flames are also summarized.

Turbulent Flames

As discussed above, temperature profiles and radiation measurements for flames burning natural gas alone are obtained during the first part of the tests. Since the operating conditions of the five tests during the first minute are also identical (to the resolution of present instruments and analysis), these data are grouped together. The five two-phase tests summarized in Table 1 are divided into two groups for the purpose of this discussion. Tests 1-3 form the first group. These involved heptane and methane burning under at almost identical conditions. Tests 4 and 5 involved Alberta sweet crude oil burning together with methane at almost identical operating conditions. These form the second group.

Methane Flames

Figure 8 shows the measurements and predictions of temperatures along the axis of the methane/air flames. The data are obtained by averaging the temperature readings from all five tests summarized in Table 1. The operating conditions are almost identical to the present approximations. The measurements have not been corrected for radiation from the thermocouple. Due to fluctuations in local flow velocities and temperatures, it is not straightforward to correct measurements in a turbulent environment for nonlinear phenomena such as radiation. The estimated corrections range between 50 to 200 K. The visual observations of the flames show liftoff from the injector exit. Although in the calculations the effects of liftoff are neglected, the predicted temperatures begin to develop at approximately $x/d = 10$ due to the potential core at the injector exit. The agreement bet-

ween the measurements and predictions in the region near the injector may be fortuitous or may suggest that the effects of liftoff do not penetrate to the flame axis. The predicted and measured temperatures are in reasonable agreement similar to past observations (Jeng and Faeth, 1984; Gore et al., 1986, 1988).

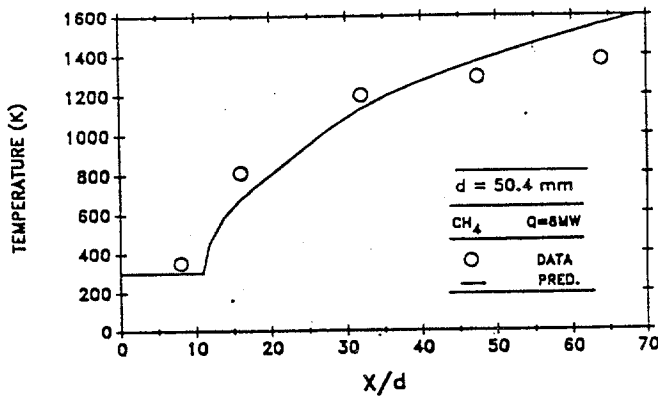


Fig. 8. Temperature Profile along the Axis of CH_4/Air Flames

Figure 9 shows measurements and predictions of total radiative heat fluxes perpendicular to the axis of the flames at a radial distance of 6.8 meters plotted as a function of normalized axial distance. The radial distance (6.8 meters is a typical measurement location and the present conclusions do not depend on this choice). The agreement between measurements and predictions is reasonably good and similar to past findings of

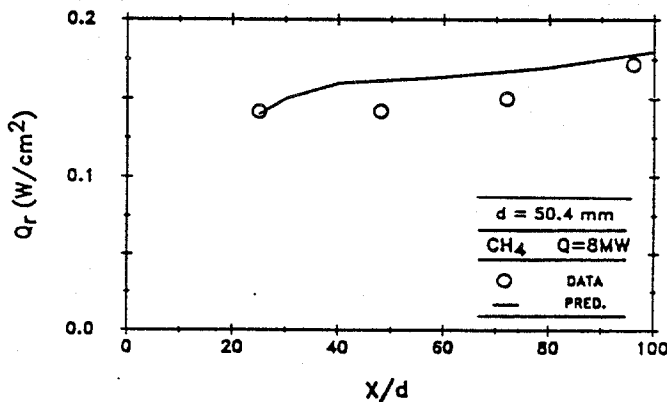


Fig. 9. Radiative Heat Fluxes Perpendicular to the Axis of CH_4/Air Flames Two Phase Flames

Jeng and Faeth(1984) and Gore et al.(1986,1988). Combined with these previous studies, the predictive capabilities of the analyses have been verified for a range of heat release rates between 0.1 MW to 100 MW. Predictions and measurements have compared favorably for heat release rates differing

by over four orders of magnitude. All predictions neglected radiation from small quantities of soot particles in the methane flames.

The two phase flames are considered next. Figure 10 shows measurements and predictions of temperatures along the axis of two-phase heptane-methane flames. Data represent averages of tests 1-3. The conclusions are not altered by the averaging between tests 1-3. Measurements have not been corrected for radiation transfer from the thermocouples as discussed before. The predicted temperatures are lower by 200 K on an average as compared to the data. The agreement is even worse if radiation corrections are considered. The difference may be due to the high sensitivity of the temperature state relationships to errors in species concentration data discussed earlier.

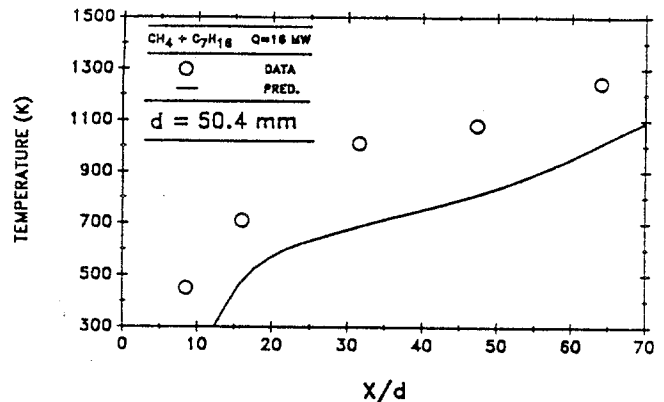


Fig. 10. Temperature Profiles along the Axis of $\text{CH}_4+\text{C}_7\text{H}_{16}/\text{Air}$ Flames

Measurements and predictions of radiative heat fluxes perpendicular to the axis of the two-phase flames are shown in Figure 11. The measured

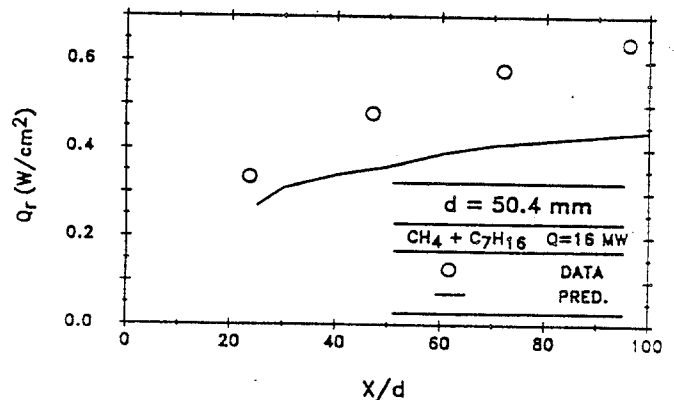


Fig. 11. Radiative Heat Fluxes Perpendicular to the Axis of $\text{CH}_4+\text{C}_7\text{H}_{16}/\text{Air}$ Flames.

radiation levels are three to six times higher than those for methane flames. Since the heat release rates are almost twice, only a part of this

increase is due to the addition of a different fuel (heptane). The analysis underpredicts the radiative heat fluxes by about thirty percent. In addition to the lower estimates of flame temperatures, approximate soot volume fractions could be a reason for this. Turbulence radiation interactions may contribute to the differences as well (Gore and Faeth, 1986, 1988; Gore, 1988). In view of the present approximations, the predictions are encouraging.

Measurements of mean temperatures along the axis and radiative heat fluxes perpendicular to the axis of flames burning Alberta sweet crude oil with methane are used to study the propriety of using heptane to simulate the crude oil in control experiments. Data from tests 4 and 5 are averaged for the purpose of this discussion. Figure 12 shows the distribution of temperatures plotted as a

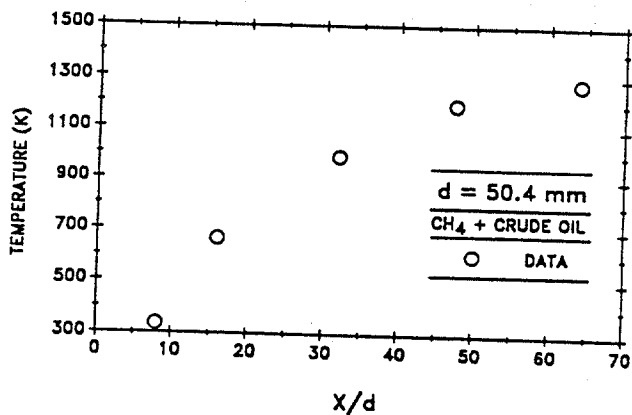


Fig. 12. Temperature Profiles along the Axis of CH₄+Alberta Sweet Crude Oil/Air Flames

function of normalized distance for the present methane-crude oil flames. The peak temperature levels are similar to those for the methane-heptane flames. The temperature profile for the crude oil flames rises more rapidly suggesting some lower boiling components.

Figure 13 shows the measurements of total radiative heat fluxes perpendicular to the axis of the present flames. The peak heat flux levels are three to six times higher than those for methane alone. This increase is similar to that observed for the methane+heptane flames. Near the injector exit, the radiative heat flux levels rise with distance at a faster rate than that seen for heptane-methane flames. This is possibly due to higher suspended solids in the crude oil. Odor of sulfur was certainly noticeable during the crude oil tests.

The temperature levels in the flames burning methane-heptane appear to be comparable to those burning methane-Alberta sweet crude oil as discussed above. If the crude oil flames produce more soot than heptane (as expected), then the reason for similar radiative heat fluxes lies in the different optical depths of the two flames. In particular, self-absorption in the methane+crude oil flames may be higher than that in the methane-

heptane flames. Measurements of soot volume fractions and global radiative loss fractions are needed to clarify this issue further.

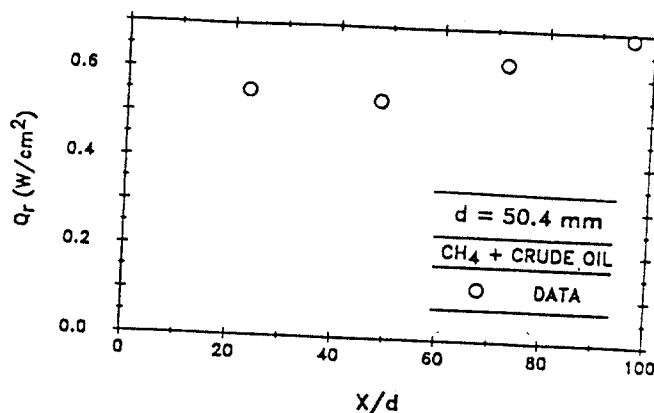


Fig. 13. Radiative Heat Fluxes Perpendicular to the Axis of CH₄+Alberta Sweet Crude Oil/Air Flames.

CONCLUSIONS

The following conclusions can be drawn from the present study:

- (1) Radiative heat fluxes around present methane air flames are predicted reasonably well, establishing scaleup capabilities of the analysis. However, those around the two-phase flames are underestimated by approximately thirty percent. The reasons include lower estimates of temperature, complexity of predicting soot in a turbulent environment, and turbulence radiation interactions.
- (2) For the present test conditions, heptane appears to be a reasonable choice for simulating Alberta-sweet crude oil in control experiments involving overall radiation properties. The similarity between the radiative fluxes from the two fuels may be due to cancelling effects of radiation emission and self absorption.

ACKNOWLEDGEMENTS

Financial support provided by the Center for Fire Research, National Institute of Standards and Technology under Grant 60NANB8D0834 is acknowledged. The experiments were performed at N.I.S.T. under funding from the Mineral Management Service of the Department of Interior with Mr. Ed Tennyson serving as Scientific Officer. The lead author also wishes to thank the Physical Plant Department, the Computer Center and the Department of Mechanical Engineering of the University of Maryland for their support.

REFERENCES

- Abdel-Khalik S.I., Tamaru, T. and El-Wakil M.M. (1975), "A Chromatographic Study of the Diffusion Flame Around a Simulated Drop," Fifteenth Symposium (International) on Combustion, The Combustion Institute, Pittsburgh, pp. 389-399.

- Becker H.A. and Liang D., 1978, "Visible Lengths of Vertical Free Turbulent Diffusion Flames," Comb. Flame, Vol. 32, pp. 115-137.
- Bilger R.W., 1977, "Reaction Rates in Diffusion Flames," Comb. Flame, Vol. 30, pp. 277-284.
- Butler T.D., Cloutman L.D., Dukowicz J.K., Ramshaw J.D. and Krieger R. B., 1980, "Toward a Comprehensive Model for Combustion in a Direct-Injection Stratified-Charge Engine," Combustion in Reciprocating Engines, J.N. Mattavi and C.A. Amanneds., Plenum, New York, pp. 231-264.
- Dalzell W. H. and Sarofim A. F., 1969, "Optical Constants of Soot and Their Application to Heat Flux Calculations," J. Heat Trans., Vol. 91, pp. 100-104.
- El Banhawy Y. E. and Whitelaw J. H., 1980, "Calculations of the Flow Properties of a Confined Kerosene-Spray Flame," AIAA J., Vol. 18, No. 12, pp. 1503-1510.
- Faeth G.M., 1977, "Current Status of Droplet and Liquid Combustion," Prog. Energy Combust. Sci., Vol. 3, pp. 191-224.
- Faeth G.M., 1983, "Evaporation and Combustion of Sprays," ibid, Vol. 9, pp. 1-76.
- Faeth G.M., 1988, "Mixing, Transport and Combustion in Sprays," ibid, Vol. 13, pp. 293-345.
- Faeth G.M., and Samuelson G.S., 1986, "Fast Reaction Non-Premixed Combustion," Prog. Energy Combust. Sci., Vol. 12, pp. 305-372.
- Gore J.P., 1988, "Coupled Structure and Radiation Analysis of Turbulent Diffusion Flames," Collected Papers in Heat Transfer, 1988, Vol. 2 (K.T. Yang ed.), ASME, New York, pp. 77-86.
- Gore J.P., Jeng S.M., and Faeth G.M., 1987a, "Spectral and Total Radiation Properties of Turbulent Carbon Monoxide /Air Diffusion Flames," AIAA J., Vol. 25, No. 2, pp. 339-345.
- Gore J.P., Jeng S.-M., and Faeth G.M., 1987b, "Spectral and Total Radiation Properties of Turbulent Hydrogen/Air Diffusion Flames," J. Heat Trans., Vol 109, No. 1, pp.165-171.
- Gore J.P. and Faeth G.M., 1986, "Structure and Spectral Radiation Properties of Turbulent Ethylene/Air Diffusion Flames," Twenty-First Symposium (International) on Combustion, The Combustion Institute, Pittsburgh, pp. 1521-1531.
- Gore J.P. and Faeth G.M., 1988, "Structure and Spectral Radiation Properties of Turbulent Acetylene/Air Diffusion Flames," J. Heat Trans., Vol. 110, No. 1, pp. 173-181.
- Gore J.P., Faeth G.M., Evans D.D. and Pfenning D.B., 1986, "Structure and Radiation Properties of Large Scale Natural Gas/Air Diffusion Flames," Fire and Materials, Vol. 10, pp. 161-169.
- Gore J.P., Evans D.D and McCaffrey B.J., 1988, "Temperature and Radiation Properties of Large Methane/Air Flames with Water Suppression," Proceedings of the Twenty-First Fall Technical Meeting of the Eastern States Section, The Combustion Institute, Pittsburgh, PA., pp. 60.1-60.4.
- Gosman A.D. and Ioannides E., 1981, "Aspects of Computer Simulation of Liquid-Fueled Combustors," AIAA Paper No. 81-0323.
- Gosman A.D., Ioannides E., Lever D.A. and Cliffe K. A., 1980, "A Comparison of Continuum and Discrete Droplet Finite-Difference Models Used in the Calculation of Spray Combustion in Swirling Turbulent Flows," AERE Harwell Report TP865.
- Grosshandler W.L. and Sawyer R.F., 1978, "Radiation from a Methanol Furnace," J. Heat Trans., Vol. 100, pp. 247-252.
- Jeng S.M. and Faeth G.M., 1984, "Radiative Heat Fluxes Near Turbulent Buoyant Methane Diffusion Flames," J. Heat Trans., Vol. 106, pp. 886-888.
- Karman D. and Steward F.R., 1984, "The Radiation Spectrum of a Test Furnace," Int. J. Heat Mass Trans., Vol. 27, pp. 1357-1364.
- Kent J. H., 1987, "Turbulent Diffusion Flame Sooting-Relationship to Smoke Point Tests," Comb. Flame, Vol. 67, pp. 223-233.
- Lockwood, F. C., and Shah, N. B., 1981, "A New Radiation Solution Method for Incorporation in General Combustion Prediction Procedures," Eighteenth Symposium (International) on Combustion, The Combustion Institute, Pittsburgh, pp. 1405-1414.
- Ludwig C.B., Malkmus W., Reardon J.E. and Thomson J.A., 1973, Handbook of Infrared Radiation From Combustion Gases, NASA SP-3080.
- Mao C.P., Szekely G.A. and Faeth G.M., 1980, "Evaluation of a Locally Homogeneous Model of Spray Combustion," J. Energy, Vol. 4, pp. 78-87.
- McCaffrey, B.J., 1986, "Momentum Diffusion Flame Characteristics and the Effects of Water Spray," NBSIR 86-3442, National Institute of Standards and Technology, Gaithersburg, MD., also Combust. Sci. and Tech., Vol. 63, pp. 315-335, 1989.
- Mitchell, R.E., Sarofim, A.F. and Clomberg L.A., 1980, "Experimental and Numerical Investigation of Confined Laminar Diffusion Flames," Comb. Flame, Vol. 37, pp. 227-234.
- Mongia, H.C. and Smith, K., 1978, "An Empirical/Analytical Design Methodology for Gas Turbine Combustors," AIAA Paper No. 78-998.
- Olson, D.B., Pickens, J.C. and Gill, R.J., 1985, "The Effects of Molecular Structure on Soot Formation II Diffusion Flames," Comb. Flame, Vol. 62, 43-60.
- Pitts, W. M., 1988, "Assessment of Theories for the Behavior and Blowout of Lifted, Turbulent Jet Diffusion Flames," Twenty Second Symposium (International) on Combustion, The Combustion Institute, Pittsburgh, PA., pp. 809-816.

Shuen J.S., Solomon, A.S.P. and Faeth G.M., 1986, "Drop-Turbulence Interactions in a Diffusion Flame," AIAA J., Vol. 24, No. 1, pp. 101-108.

Spalding D.B., 1977, GENMIX: A General Computer Program for Two-Dimensional Parabolic Phenomena, Pergamon Press, Oxford.

Swithenbank J., Turan A. and Felton P.G., 1980, "Three-Dimensional Two-Phase Mathematical Modelling of Gas Turbine Combustors," Gas Turbine Combustor Design Problems, A. H. Lefebvre ed., Hemisphere, Washington, pp. 249-314.

Tsuji, H. and Yamaoka, I., 1969, "The Structure of Counterflow Diffusion Flames in the Forward Stagnation Region of a Porous Cylinder," Twelfth Symposium (International) on Combustion, The Combustion Institute, Pittsburgh, PA, pp. 997-1005.

